THE JOURNAL OF BIOLOGICAL CHEMISTRY VOL. 287, NO. 33, pp. 28112–28121, August 10, 2012

A Novel Nuclear Trafficking Module Regulates the Nucleocytoplasmic Localization of the Rabies Virus Interferon Antagonist, P Protein*[S]

Received for publication, May 15, 2012, and in revised form, June 13, 2012 Published, JBC Papers in Press, June 14, 2012, DOI 10.1074/jbc.M112.374694

Sibil Oksayan[‡§], **Linda Wiltzer**[‡§], **Caitlin L. Rowe**[‡§], **Danielle Blondel**[¶], **David A. Jans**[§], **and Gregory W. Moseley**[‡1]

From the [‡]*Viral Immune Evasion and Pathogenicity Laboratory and* [§]*Nuclear Signaling Laboratory, Department of Biochemistry and Molecular Biology, Monash University, 3800 Victoria, Australia and the* [¶]*Laboratoire de Virologie Moléculaire et Structurale, Centre de Recherche de Gif, CNRS 91198 Gif-sur-Yvette, France*

Background: Rabies virus expresses five isoforms of P protein, which undergo nucleocytoplasmic trafficking important to roles as antagonists of interferon-mediated immunity.
Results: P isoform trafficking is mediated by a novel module containing co-regulated overlapping nuclear localization and export signals.
Conclusion: P isoform nuclear localization involves a novel trafficking module.
Significance: A novel molecular switch regulating trafficking, important to a viral interferon antagonist, is identified.

Regulated nucleocytoplasmic transport of proteins is central to cellular function and dysfunction during processes such as viral infection. Active protein trafficking into and out of the nucleus is dependent on the presence within cargo proteins of intrinsic specific modular signals for nuclear import (nuclear localization signals, NLSs) and export (nuclear export signals, NESs). Rabies virus (RabV) phospho (P) protein, which is largely responsible for antagonising the host anti-viral response, is expressed as five isoforms (P1–P5). The subcellular trafficking of these isoforms is thought to depend on a balance between the activities of a dominant N-terminal NES (N-NES) and a distinct C-terminal NLS (C-NLS). Specifically, the N-NES-containing isoforms P1 and P2 are cytoplasmic, whereas the shorter P3–P5 isoforms, which lack the N-NES, are believed to be nuclear through the activity of the C-NLS. Here, we show for the first time that RabV P contains an additional strong NLS in the N-terminal region (N-NLS), which, intriguingly, overlaps with the N-NES. This arrangement represents a novel nuclear trafficking module where the N-NLS is inactive in P1 but becomes activated in P3, concomitant with truncation of the N-NES, to become the principal targeting signal conferring nuclear accumulation. Understanding this unique switch arrangement of overlapping, co-regulated NES/NLS sequences is vital to delineating the critical role of RabV P protein in viral infection.

The eukaryotic cell nucleus is separated from the cytoplasm by the double-membrane nuclear envelope. All transport across the nuclear envelope occurs through nuclear pore complexes, and active protein transport through the nuclear pore complexes is dependent on nuclear localization signals (NLSs)[2] or nuclear export signals (NESs) within the cargo proteins (1–4). This enables the specific regulation of protein access to the nuclear contents including the genomic DNA, an essential mechanism in processes such as development, apoptosis, and immunity (for review, see Refs. 1, 3, 5).

NLS/NES-dependent trafficking is mediated by importin (IMP) proteins, of which there are at least 6 α and 24 β isoforms in humans. IMPs bind directly to NLSs/NESs, either as an IMPα/β1 heterodimer or as an IMPβ homologue alone (6–8). NLSs are commonly short monopartite or bipartite sequences enriched in basic residues (9–11); classical monopartite NLSs such as the SV40 large T-antigen (T-ag) NLS are single short basic sequences that variously conform to the KK*X*K consensus sequence (where *X* is any amino acid) (12), whereas bipartite NLSs typically contain two stretches of 4–8 basic residues separated by a 10–12-residue spacer (9, 10). Recent studies have also identified a number of nonclassical bipartite NLSs with longer spacers (up to 30 residues) (9, 13), as well as conformation-dependent NLSs such as that of the signal transducer and activator of transcription 3 (STAT3) (11). NESs are typically 9–15-residue sequences containing a conserved hydrophobic residue motif (7) and are recognized by exportins of the IMPβ superfamily, the best characterized of which is CRM1.

NLSs and NESs are generally functionally independent, modular sequences able to mediate active nuclear import or export of heterologous proteins (12, 14, 15). Thus, the addition/deletion of independent modular NLSs or NESs by mechanisms including alternate mRNA splicing, leaky ribosomal mRNA scanning, and RNA editing, represents a key mechanism by which differential nucleocytoplasmic localization can be con-

* This work was supported by National Health and Medical Research Council, Australia, Project Grant 1003244 (to G. W. M.), and Senior Principal Research Fellowship 1002486 (to D. A. J.), and by Australian Research Council Discovery Project DP110101749 (to G. W. M. and D. A. J.).
[S] This article contains supplemental Fig. S1.
[1] To whom correspondence should be addressed. Tel.: 61-3-9902-9354; Fax: 61-3-9902-9500; E-mail: greg.moseley@monash.edu.

[2] The abbreviations used are: NLS, nuclear localization signal; C-NLS, NLS in the C-terminal domain; CLSM, confocal laser scanning microscopy; DLC-AS, dynein light chain-association sequence; IMP, importin; LMB, leptomycin-B; MTAS, microtubule-association sequence; NES, nuclear export signal; N-NES, NES close to the N terminus; N-NLS, NLS in the N-terminal region; PML, promyelocytic leukemia; RabV, rabies virus; T-ag, T-antigen.

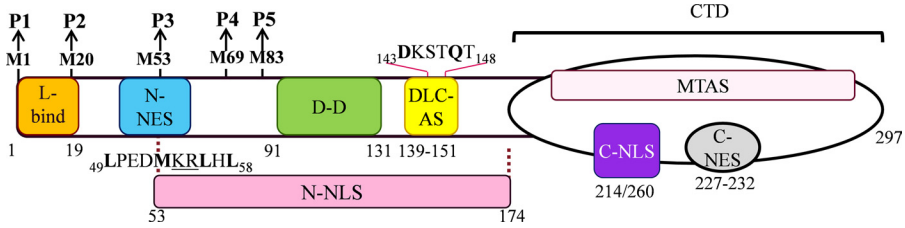

FIGURE 1. **Schematic representation of RabV P protein.** The RabV P gene encodes a 297-residue protein (P1) and four N-terminally truncated isoforms (P2–P5), expressed from internal in-frame AUG start codons encoding methionine (M) residues at positions 20, 53, 69, and 83 (19). RabV P interacts with the cellular trafficking machinery through the N-NES (sequence indicated under the protein with key residues in *bold*) and C-NES, which interact with CRM1, and the C-NLS (the critical residues of which include Lys^{214}/Arg^{260}, which are proximally localized on the CTD surface) (30, 42) and N-NLS (identified in the current study; critical residues of the N-NLS within the N-NES sequence are *underlined*). RabV P nuclear import is facilitated by interactions with the dynein light chain LC8 via a DLC-AS (sequence indicated above protein with essential residues Asp^{143}/Gln^{147} in *bold*) (44, 66). A MTAS, mapped within the C-terminal domain (*CTD*), also enables association of P3 with the MT network (43). The N-NES is truncated in P3 to remove residues 49–52 and is deleted from P4 and P5, enabling nuclear localization of these isoforms. RabV P also interacts with viral proteins L (via P^{1-19}) and N (not shown) (67, 68), homodimerizes via the dimerization domain (D-D) (58), and interacts with cellular proteins of the IFN system such as STAT 1 and 2, and PML (not shown) (37, 39). The positions of individual domains are indicated by *residue numbers* beneath the protein.

ferred on the isoforms of cellular proteins including promyelocytic leukemia (PML) protein, Krüppel-like factor 6, and spastin (16–18), as well as virus-encoded proteins such as RabV P and paramyxovirus P/V/W proteins (19–21); this is thought to play key roles in isoform functional heterogeneity.

Regulated nuclear trafficking of viral proteins is common even for viruses with entirely cytoplasmic life cycles such as RabV (22–30), as it enables viral modification of host cell functions through interference with intranuclear processes and/or the nucleocytoplasmic trafficking of cellular proteins (31–34). RabV P protein is expressed as five isoforms in infected cells, full-length P1 and the N-terminally truncated P2–P5 (Fig. 1), which perform functions in viral replication processes and antagonism of interferon (IFN)-mediated antiviral responses (19, 29, 35–38). P1 is the most abundantly expressed isoform, presumably enabling essential roles as the viral polymerase (L-protein)-binding co-factor, whereas the "accessory" proteins P2–P5 show a decreasing gradient of expression (19, 29). P isoform nuclear trafficking has been reported to play vital roles in IFN antagonism by enabling cytoplasmic and nuclear targeting of essential factors of the IFN system including STAT1 and 2, to affect their nucleocytoplasmic trafficking/DNA binding, and PML nuclear bodies (29, 35–39). As a result, defects in the trafficking of RabV P correlate with defective viral IFN antagonism and pathogenicity in infected animals (36, 40). Analogous functions have been attributed to isoforms of the vesicular stomatitis virus M protein, and of the P proteins of Nipah and Hendra viruses (21, 24–29, 41). Thus, the expression of multiple isoforms with heterogeneous nucleocytoplasmic localization appears to be an important mechanism whereby viruses with limited genome capacity can optimize their functional proteome to enable efficient evasion of the IFN response (29).

RabV P isoform nucleocytoplasmic localization is currently believed to be determined principally by two distinct, independent signals: a dominant CRM1-dependent NES close to the N terminus (N-NES, residues 49–58) and a predicted NLS (C-NLS) in the C-terminal domain (CTD; Fig. 1) (30). P1 and P2 contain the N-NES and are thus cytoplasmic (30). In contrast, P3–P5 can localize in the nucleus, and this is thought to be due to truncation/deletion of the N-NES such that the C-NLS becomes the main "default" targeting signal (Fig. 1) (30). However, the nucleocytoplasmic localization of RabV P isoforms and the NLS function of P with regard to IMP binding have never been quantitatively examined. Using single cell imaging approaches and *in vitro* molecular interaction analyses, we have examined the trafficking of P protein in detail, finding that the nucleocytoplasmic localization of P isoforms is principally regulated by a novel nuclear trafficking module in which the N-NES overlaps with a newly identified N-terminal NLS (N-NLS) sequence (Fig. 1). The close association of these signals enables their co-regulation by a unique mechanism whereby truncation of the module both inactivates the N-NES and concomitantly activates the N-NLS, producing a coordinated effect on protein trafficking. This work reveals a novel mechanism underlying the efficient regulation of protein nuclear trafficking, and contributes to our understanding of events at the virus-host interface.

EXPERIMENTAL PROCEDURES

Constructs—All P protein constructs were generated using the P gene from RabV CVS11 strain, as described previously (42–44). cDNA encoding P isoforms or truncated derivatives was generated by PCR and cloned in-frame N-terminal to GFP in the pEGFP-N3 vector by BglII-BamHI restriction ligation (42–44) for the expression of GFP-fused protein in mammalian cells. To express untagged proteins, the cDNA was cloned into the pΔEGFP-C1 vector, which we generated by excising GFP from the pEGFP-C1 vector using BspE1 and AgeI. cDNA containing mutations to residues Lys^{54}, Arg^{55}, Asp^{143}, Gln^{147}, Lys^{139}, and Arg^{144} (positions of the residues in the P protein sequence are shown in superscript) was generated by PCR extension or overlap mutagenesis as described previously (42, 44). Constructs for the expression of His_6-tagged GFP fusion proteins in *Escherichia coli* used the pGFP-RfB vector, and were generated using the Gateway™ Cloning System (Invitrogen) (23, 45).

Cell Culture, Transfection, Drug Treatments, and Immunofluorescence—HeLa cells were routinely cultured in DMEM with 10% FCS (37 °C, 5% CO_2). For confocal laser scanning microscopy (CLSM), cells were grown on coverslips to 80–90% confluence before transfection using Lipofectamine 2000 (Invitrogen) and analysis 16–24 h later. For inhibition of CRM1-mediated nuclear export, cells were treated with 2.8

ng/ml leptomycin-B (LMB, a kind gift from M. Yoshida, RIKEN, Japan) for 3 h prior to analysis.

For indirect immunofluorescence of untagged protein, cells were washed with PBS and fixed using 3.7% formaldehyde followed by 90% methanol (43). Cells were then blocked in 1% BSA in PBS before immunostaining with anti-RabV P protein antibody (46) and Alexa Fluor 488-coupled secondary antibody (Invitrogen A11008).

CLSM and Image Analysis—Cells were analyzed using a Nikon Eclipse C1 inverted confocal laser scanning microscope, with an Olympus 60× oil immersion objective (NA 1.4) (for fixed cells) or an Olympus 60× water immersion objective (NA 1.2) and 37 °C heated chamber (for living cells). Analysis of digitized CLSM images was performed using ImageJ software (v1.44p) as described previously (42–44, 47–49) to determine the ratio of nuclear to cytoplasmic fluorescence ($F_{n/c}$) for single cells using the formula $F_{n/c} = (F_n - F_b)/(F_c - F_b)$, where F_n is the nuclear fluorescence, F_c the cytoplasmic fluorescence, and F_b the background fluorescence. The mean $F_{n/c}$ was calculated for ≥49 cells, and statistical analysis (*t* test) was performed using GraphPad Instat software as described previously (42).

Protein Expression and Purification—Constructs encoding His_6-tagged GFP-fused P protein derivatives P^{54-174} and P^{1-174} (sequence of P indicated in superscript), and P^{54-174}-(K54N/R55N) (in which Lys^{54} and Arg^{55} are mutated to asparagine) were expressed in *E. coli* strain BL21 pRep4 cells before induction of expression and purification using nickel-nitrilotriacetic acid columns (Qiagen) under denaturing conditions (8 M urea), as described previously (50). Proteins were renatured on the column and eluted with 200 mM imidazole (45), prior to dialysis and concentration using a 30K MWCO column (Amicon). Mouse IMPα2 and IMPβ1 were expressed as GST fusion proteins and purified by affinity chromatography using glutathione-Sepharose (50); biotinylated IMPα2 protein generated as described previously (51), and GFP-T-ag-NLS protein, were kindly donated by Dr. Kylie Wagstaff (Monash University. Australia).

Native Gel Electrophoresis—GFP fusion proteins (2 μM) were incubated with or without IMPα2, IMPβ1, or predimerized IMPα/β (1–9 μM), for 15 min at room temperature and then electrophoresed for 3–5 h at 4 °C in 1× TBE buffer using precast native polyacrylamide (10%) gels (Bio-Rad) (52). The migration of GFP fusion proteins was visualized using a Typhoon™ Trio Variable Mode Imager (GE Life Sciences), and gel images were processed using ImageJ software as described previously (52).

AlphaScreen Binding Assays—GFP-fused P proteins (30 nM final concentration) and 0–60 nM biotinylated IMPα2 or IMPα/β heterodimer were incubated in 384-well plates (PerkinElmer Life Sciences) for 30 min at room temperature. 1 μl of streptavidin-coated acceptor beads (diluted 1:10 in PBS) and 1 μl of 2.5% BSA in PBS were then added to each well (51). After 90 min, 1 μl of nickel chelate-coated donor beads (diluted 1:10 in PBS) was added and incubated for a further 2 h before measurement of AlphaScreen counts using a Fusion-α™ plate reader (PerkinElmer Life Sciences) (51). Triplicate values were averaged and curves plotted using SigmaPlot (51).

RESULTS

P3 Nuclear Localization Is Significantly Greater Than That of Other Isoforms—Previous research using nonquantitative CLSM analysis of fixed cells indicated that P1 and P2 are cytoplasmic due to the N-NES, whereas P3–P5 are mostly nuclear due to the C-NLS (30). This work also indicated that the level of nuclear localization may differ among P3, P4, and P5, implying that additional sequences or mechanisms contribute to trafficking. To determine quantitatively the nucleocytoplasmic distribution of P1–P5, we transfected HeLa cells to express these proteins fused at their C termini to GFP, enabling analysis of their localization in living cells by CLSM (Fig. 2*A*). P1-GFP and P2-GFP were clearly excluded from the nucleus, whereas P4-GFP and P5-GFP could enter cell nuclei but showed only moderate nuclear localization. P3-GFP, however, showed clear nuclear accumulation (Fig. 2*A*). To quantitate the nuclear localization, we determined the nuclear to cytoplasmic fluorescence ratio ($F_{n/c}$) as previously (42–44, 47–49) (Fig. 2*C*), confirming that P1- and P2-GFP were both excluded almost entirely from the nucleus ($F_{n/c}$ of approximately 0.2), whereas P4- and P5-GFP both exhibited diffuse localization ($F_{n/c}$ of approximately 1) similar to that of GFP alone. In contrast, the level of accumulation of P3-GFP ($F_{n/c}$ of approximately 7), was approximately 5-fold higher than that of P4-GFP (Fig. 2*C*). Comparable results were observed in Vero cells (data not shown).

We also examined the localization of untagged P protein isoforms in transfected HeLa cells by fixation and immunostaining with anti-P antibody before quantitative CLSM analysis (Fig. 2, *B* and *D*). This confirmed the observations from live-cell analyses, showing that P3 accumulates in the nucleus to a much greater extent than the other isoforms (Fig. 2*D*).

P3–P5 each lack the N-NES and contain the C-NLS that is predicted to mediate nuclear localization of these isoforms (30), as well as a CRM1-dependent NES in the CTD (C-NES), which can modulate nuclear localization by the C-NLS (42) (Fig. 1). Thus, the differential nuclear trafficking of P3–P5 could indicate that the C-NLS is a relatively weak signal and that P3 contains an additional, stronger NLS, or that the activity of the C-NES is increased in P4 and P5 compared with P3. To test this, we treated cells expressing GFP-fused P isoforms with or without the CRM1 inhibitor LMB before analysis by CLSM (42) (Fig. 2*A*). LMB treatment significantly increased the nuclear localization of all GFP-fused P isoforms but not that of GFP alone, confirming that the localization of all P isoforms is regulated by CRM1, due to the N-NES and/or C-NES (Fig. 2, *A* and *C*) (42). However, even in LMB-treated cells, P3-GFP nuclear accumulation remained much higher (>7-fold) than that of P4- or P5-GFP (Fig. 2*C*). Intriguingly, the $F_{n/c}$ for P3-GFP was also approximately 10-fold that for P1-GFP, even though P1 contains the entire P3 sequence. Thus, it appeared that P3 contains a previously uncharacterized NLS that is inactive in P1 due to the presence of P protein residues 1–52, and absent or inactivated in P4 and P5 due to the deletion of the residues 53–68 (Fig. 1).

P3 Contains a NLS in Its N-terminal Region—To determine the minimal region of P3 sufficient to account for its increased nuclear localization compared with other isoforms, we gener-

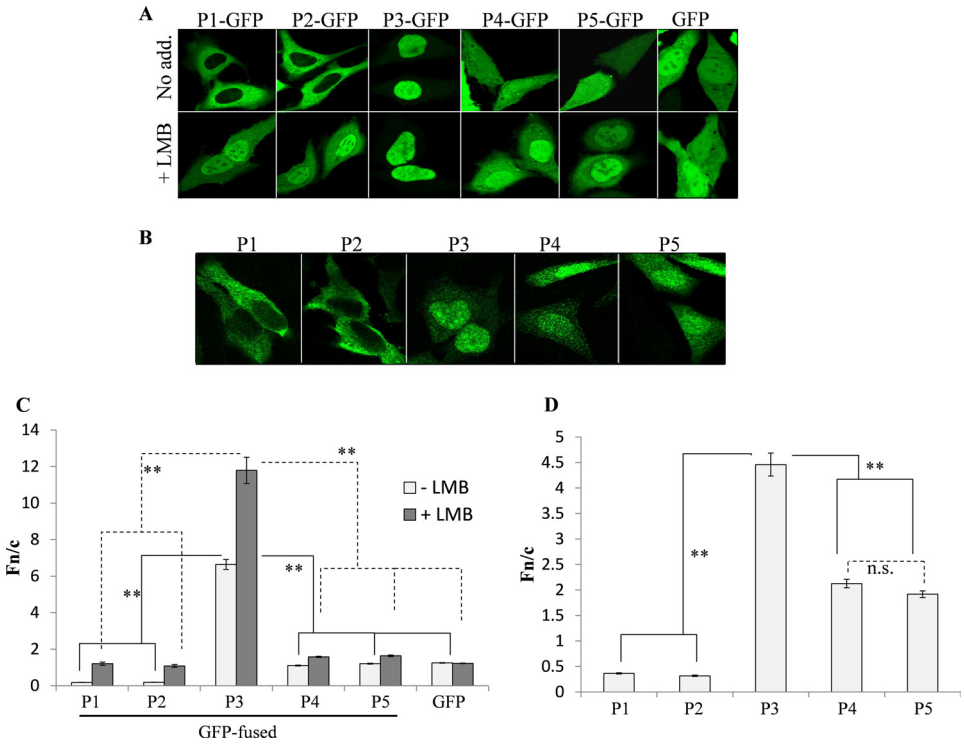

FIGURE 2. **P3 is more nuclear than other P isoforms due to differing nuclear import.** *A* and *B*, HeLa cells transfected to express the indicated proteins were treated with or without LMB (2.8 ng/ml, 3 h) prior to imaging of living cells by CLSM (*A*), or fixation and immunostaining of cells with anti-P antibody for CLSM analysis (*B*). *C* and *D*, images such as those shown in *A* and *B* were analyzed to determine the ratio of nuclear to cytoplasmic fluorescence ($F_{n/c}$) as described previously (36, 42–44, 47, 48). Data are shown as mean $F_{n/c} \pm$ S.E. (*error bars*), $n \geq 52$ from ≥ 2 separate assays. Statistical analysis used Student's *t* test (unpaired) (**, $p < 0.0001$; *n.s.*, not significant).

ated several C-terminally truncated versions of P3 fused to GFP and determined their subcellular localization in living HeLa cells as above (Fig. 3*A*).

P^{53-68}-GFP and P^{53-81}-GFP (encoding the P protein residues indicated in superscript) correspond to the regions deleted from P4 and P5 respectively compared with P3. Both regions contain several basic residues that could form part of a NLS (Lys^{54}, Arg^{55}, Lys^{62}, Arg^{70}, Arg^{77}), and NLSmapper online prediction software (53) indicated that P^{53-81} may contain a bipartite NLS (data not shown). However, both regions failed to confer nuclear accumulation on GFP (Fig. 3, *A* and *C*; $F_{n/c}$ of approximately 1), indicating that additional sequence is required. The minimal region able to confer nuclear accumulation on GFP was within P^{53-139}, which showed an $F_{n/c}$ value of approximately 2.5 (Fig. 3, *A* and *C*); this level of nuclear accumulation, however, was not as high as that of P3.

P^{53-151} and P^{53-174} both contain the RabV P dynein light chain-association sequence (DLC-AS) (see Fig. 1), which facilitates NLS-mediated nuclear import (44, 49). P^{53-151}-GFP accumulated in the nucleus to a significantly ($p < 0.0001$) higher extent ($F_{n/c}$ of approximately 6) than P^{53-139}-GFP, but to a significantly ($p = 0.0156$) lower extent than P3-GFP ($F_{n/c} > 7$) (Fig. 3, *A* and *C*). In contrast, P^{53-174}-GFP ($F_{n/c}$ of 7.5) accumulated in the nucleus to levels completely in keeping with those of P3-GFP (Fig. 3, *A* and *C*), indicating that P^{53-174} contains the sequence necessary and sufficient to mediate full nuclear localization of P3. This sequence was named the N-terminal NLS (N-NLS).

Importantly, P^{53-174} lacks the C-NLS/C-NES-containing CTD (Fig. 1), indicating that the predicted C-NLS makes little or no contribution to P3 nuclear accumulation. To test this, we compared the nuclear accumulation of P^{53-174}-GFP with that of the CTD ($P^{173-297}$-GFP), in cells treated with or without LMB (Fig. 3, *B* and *D*). P^{53-174} conferred significantly ($p < 0.0001$) higher nuclear accumulation (4-fold) on GFP than did the CTD. Further, this difference was almost 7-fold in LMB-treated cells (Fig. 3, *B* and *D*), indicating that the N-terminal region/N-NLS makes a greater contribution to the nuclear import of P3 than the CTD/C-NLS.

Identification of Residues Important for P3 Nuclear Accumulation—Because P3 accumulates in the nucleus to a significantly higher extent than P4 (see above), P^{53-68} is likely to contain key residues of the N-NLS. As NLSs commonly contain clustered basic residues, we tested the role of Lys^{54} and Arg^{55} in P3 nuclear accumulation by generating constructs for the expression of GFP-fused P protein derivatives in which these residues were mutated to asparagine: P3-(K54N/R55N)-GFP and P^{53-174}-(K54N/R55N)-GFP, in which both residues are mutated, and P3-(K54N)-GFP, P^{53-174}-(K54N)-GFP, P3-(R55N)-GFP and P^{53-174}-(R55N)-GFP, which contain single mutations. CLSM analysis of live HeLa cells expressing these proteins (Fig. 4, *A* and *B*) indicated that both residues are important for nuclear localization of P3 and P^{53-174}, as mutation of either residue individually or their combined mutation, resulted in a significant decrease in nuclear accumulation compared with wild-type (WT) protein (Fig. 4*B*). No significant difference in $F_{n/c}$ was found between proteins containing either the K54N or R55N single mutations, or the K54N/R55N double mutation ($F_{n/c}$ values of approximately 0.8 in all cases), indicating that both residues are critical to the N-NLS. Similar effects

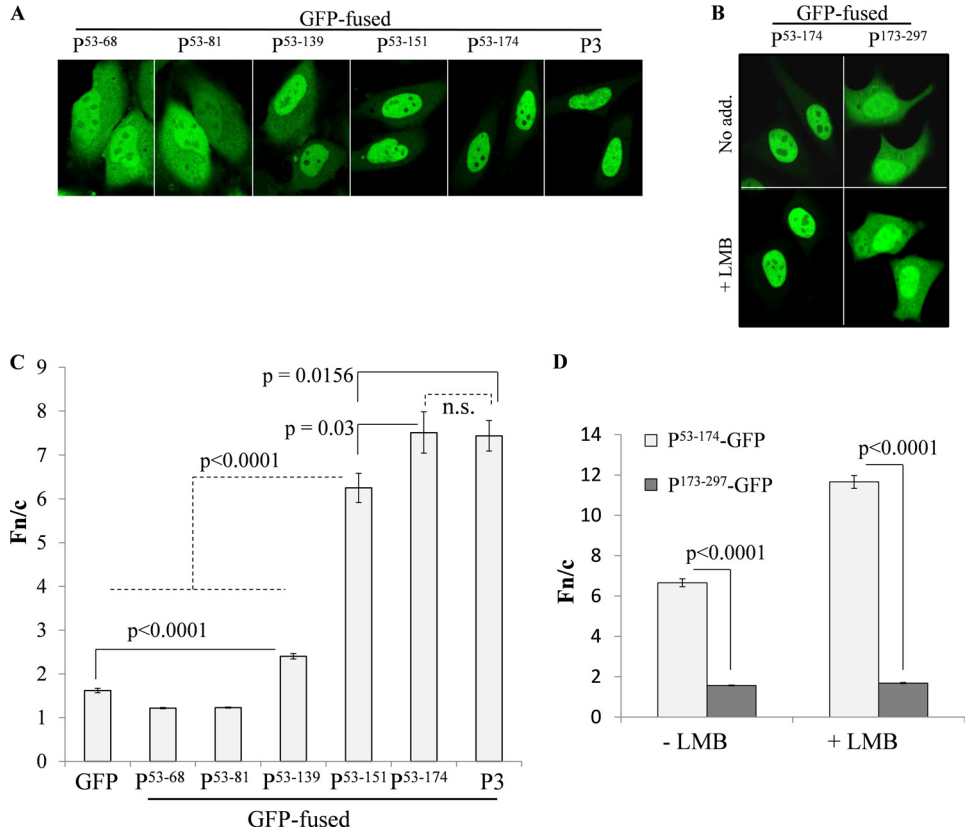

FIGURE 3. **P^{53-174} is necessary and sufficient to confer nuclear accumulation equivalent to that of P3.** *A* and *B*, HeLa cells were transfected to express the indicated proteins. *C* and *D*, live cells, treated with or without LMB, were analyzed by CLSM to calculate the $F_{n/c}$ (mean ± S.E. (*error bars*), $n \geq 49$ from 3 separate assays), as described in the legend to Fig. 2. Statistical analysis was according to the legend to Fig. 2 with *p* values indicated (*n.s.*, not significant).

were observed for constructs in which residues Lys^{54} and Arg^{55} were deleted (data not shown), and a similar decrease in nuclear accumulation was observed in fixed, immunostained cells transfected with untagged P3-(K54N/R55N) compared with WT P3 ($F_{n/c}$ of approximately 2 and 5 respectively; images not shown). Thus, Lys^{54}/Arg^{55} are essential to N-NLS function, and their proximity to the N terminus may account for the quantitatively lower levels of nuclear accumulation observed in previous studies using P3 modified at its N terminus (42, 43).

To investigate directly the potential role of the DLC-AS in facilitating N-NLS-mediated nuclear import, we converted the essential DLC-AS residues Asp^{143} and Gln^{147} to alanine in P3 and P^{53-174} (P3-(D143A/Q147A)-GFP and P^{53-174}-(D143A/Q147A)-GFP, respectively), which has been shown to inhibit DLC-AS-facilitated nuclear import (44, 54). The mutations resulted in a significant decrease in nuclear accumulation of GFP-fused P3 and P^{53-174} proteins (Fig. 4, *C* and *D*). However, they did not reduce the $F_{n/c}$ of P^{53-174}-GFP to a level equivalent to that of P^{53-139}-GFP, indicating that the region $P^{139-174}$ contains additional sequence(s) that contribute to P3 nuclear localization, potentially including basic residues forming part of the N-NLS sequence. To examine this, we analyzed the nucleocytoplasmic localization of P3-GFP carrying mutations to asparagine of the residues Lys^{139} and Arg^{144}, which show high conservation between the P proteins of RabV strains and related lyssaviruses (data not shown). Live-cell CLSM analysis revealed no significant difference between the levels of nuclear accumulation of P3-(K139N)-GFP and WT P3-GFP ($F_{n/c}$ of approximately 8 in both cases), with mutation of both residues resulting in only a moderate decrease ($F_{n/c}$ of approximately 6; images not shown). This indicated that Arg^{144} makes a contribution to P3 nuclear accumulation, but that other residues are important, and residues, Lys^{54} and Arg^{55} are essential. Importantly, the fact that Lys^{54} and Arg^{55} are located within the N-NES indicates a physical overlap of sequences critical to the N-NES and N-NLS (Fig. 1).

The P3 N-NLS Is Recognized by the IMPα/β Heterodimer with High Affinity—The above data indicate that P^{53-174} contains a previously unidentified NLS (N-NLS) that is responsible for the high nuclear accumulation of P3. To confirm that this region contains an IMP-recognized NLS (10), we tested the binding of purified recombinant GFP-fused proteins encoding the regions P^{54-174} and P^{54-174}-(K54N/R55N) to GST-fused IMPα2 and IMPβ1 proteins (see supplemental Fig. S1), initially using native PAGE as described previously (50–52, 55–57) (Fig. 5).

GFP-P^{54-174} interacted with both IMPα2 and the IMPα/β dimer, as indicated by a change in the mobility in the native gel compared with in the absence of IMP addition, which was comparable with that observed for the well characterized IMPα/β-binding NLS of T-ag (50–52) (Fig. 5*A*). Consistent with the idea that Lys^{54} and Arg^{55} are critical to the N-NLS, mutation of these residues diminished the IMP interactions. Although there was some interaction of the proteins with GST-IMPβ1, this was to a markedly lower extent than with GST-IMPα or GST-IMPα/β, implying that P3 nuclear transport is likely to rely on the IMPα/β heterodimer. Native PAGE was also used to

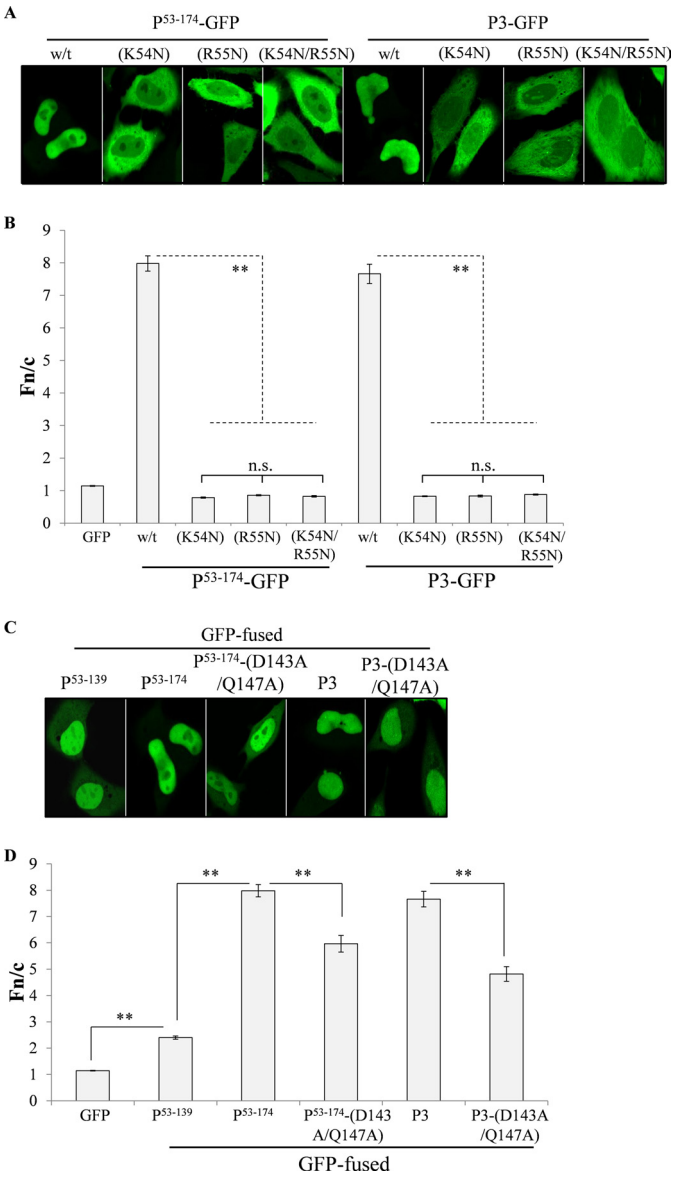

FIGURE 4. **P3 nuclear accumulation is critically dependent on residues Lys^{54} and Arg^{55} and is facilitated by the DLC-AS.** *A* and *C*, HeLa cells transfected to express the indicated proteins were analyzed live by CLSM. *B* and *D*, images such as those shown were analyzed to determine the $F_{n/c}$ (mean ± S.E. (*error bars*), $n \geq 57$ from three separate assays) as described in the legend to Fig. 2. *w/t*, wild-type. Statistical analysis was according to the legend to Fig. 2.

analyze binding of increasing amounts of GST-IMPα2 (Fig. 5*B*) or GST-IMPα/β heterodimer (Fig. 5*C*), results confirming markedly reduced binding to GFP-P$^{54-174}$-(K54N/R55N) of IMPα and IMPα/β compared with GFP-P$^{54-174}$. Notably, GFP-P$^{54-174}$ showed a strong shift in mobility at concentrations of 1–2 μM IMPα/β, whereas a similar shift was only observed at 8–9 μM in the case of IMPα, consistent with the idea that P$^{54-174}$ contains a classical IMPα/β-recognized NLS, where high affinity binding of IMPα is dependent on heterodimerization with IMPβ (see 22, 50, 52).

We also used the highly sensitive AlphaScreen assay to analyze binding (51), results indicating high affinity binding of IMPα/β to GFP-P$^{54-174}$ (apparent dissociation constant, K_d, of 0.8 ± 0.15 nM) (Fig. 5*D*). Analysis also revealed that maximal binding (B_{max}) of GFP-P$^{54-174}$-(K54N/R55N) to IMPα/β was markedly lower than that of GFP-P$^{54-174}$ (Fig. 5*D*). These data indicate that residues Lys^{54} and Arg^{55} are critical for IMP binding, representing the basis for the effects on nuclear transport efficiency observed in Fig. 4.

The N-terminal 52 Residues of P1 Inhibit N-NLS Activity—The above data indicate that P3 contains a functional N-NLS that is inactivated by the deletion of key residues from P4 and P5, accounting for the difference in nuclear localization of these isoforms. However, P1 contains the entire N-NLS sequence, but remains substantially less nuclear than P3 in cells treated with or without LMB (Fig. 2, *A* and *C*). This implies that the N-NLS is inhibited in the context of P1, through the presence of residues P$^{1-52}$. To examine this, we performed native PAGE and AlphaScreen analyses to examine the binding of GFP-P$^{1-174}$ to IMPα2 and the IMPα/β heterodimer as above (Fig. 5). Binding of both IMPα and IMPα/β to GFP-P$^{1-174}$ was profoundly decreased compared with GFP-P$^{54-174}$, such that little or no shift was evident in the native gels (Fig. 5, *B* and *C*). Quantitative analysis using AlphaScreen (Fig. 5*D*) confirmed this observation, with a B_{max} for GFP-P$^{1-174}$ binding to IMPα/β that was markedly decreased compared with that for GFP-P$^{54-174}$. Clearly, the N-terminal 53 residues of P inhibit IMP binding to the N-NLS *in vitro*.

To confirm that the nuclear targeting function of the N-NLS is inhibited by residues P$^{1-52}$ *in vivo*, we expressed P$^{1-174}$-GFP and P$^{53-174}$-GFP as well as P1-GFP, P3-GFP, and mutated versions thereof, in HeLa cells and imaged them live by CLSM (Fig. 6). Quantitative analysis indicated that P$^{53-174}$-GFP showed almost 10-fold higher nuclear targeting ability than P$^{1-174}$-GFP in cells treated either without or with LMB (Fig. 6, *A* and *B*). Importantly, although mutation of Lys^{54} and Arg^{55} significantly ($p < 0.0001$) diminished P3-GFP nuclear accumulation, it had negligible effect on nuclear localization of P1-GFP in cells treated either without or with LMB (Fig. 6, *C* and *D*), implying that the N-NLS plays no role in P1 nuclear import. Together, these data indicate that the N-NLS is inhibited in P1 by residues P$^{1-52}$, and that, in a unique mechanism, truncation of these residues concomitantly inactivates the N-NES and activates the N-NLS to effect strong nuclear accumulation of P3.

DISCUSSION

Here we show definitively for the first time that RabV P protein contains a novel trafficking module, incorporating overlapping NES and NLS sequences, representing the basis of a unique regulatory mechanism. Specifically, residues P$^{1-52}$ form part of the functional N-NES, but directly inhibit the function of the N-NLS sequence (identified for the first time in this study), to effect robust nuclear exclusion of the P1 isoform. Truncation of the module in P3 by deletion of P$^{1-52}$ inactivates the N-NES and activates the N-NLS *de novo*, resulting in strong nuclear accumulation. Thus, this module enables the highly coordinated regulation of opposing nuclear trafficking sequences. This mechanism differs fundamentally from the previously accepted model of regulation of P protein isoform nuclear trafficking through the differential expression of distinct, functionally independent trafficking signals (30) and rep-

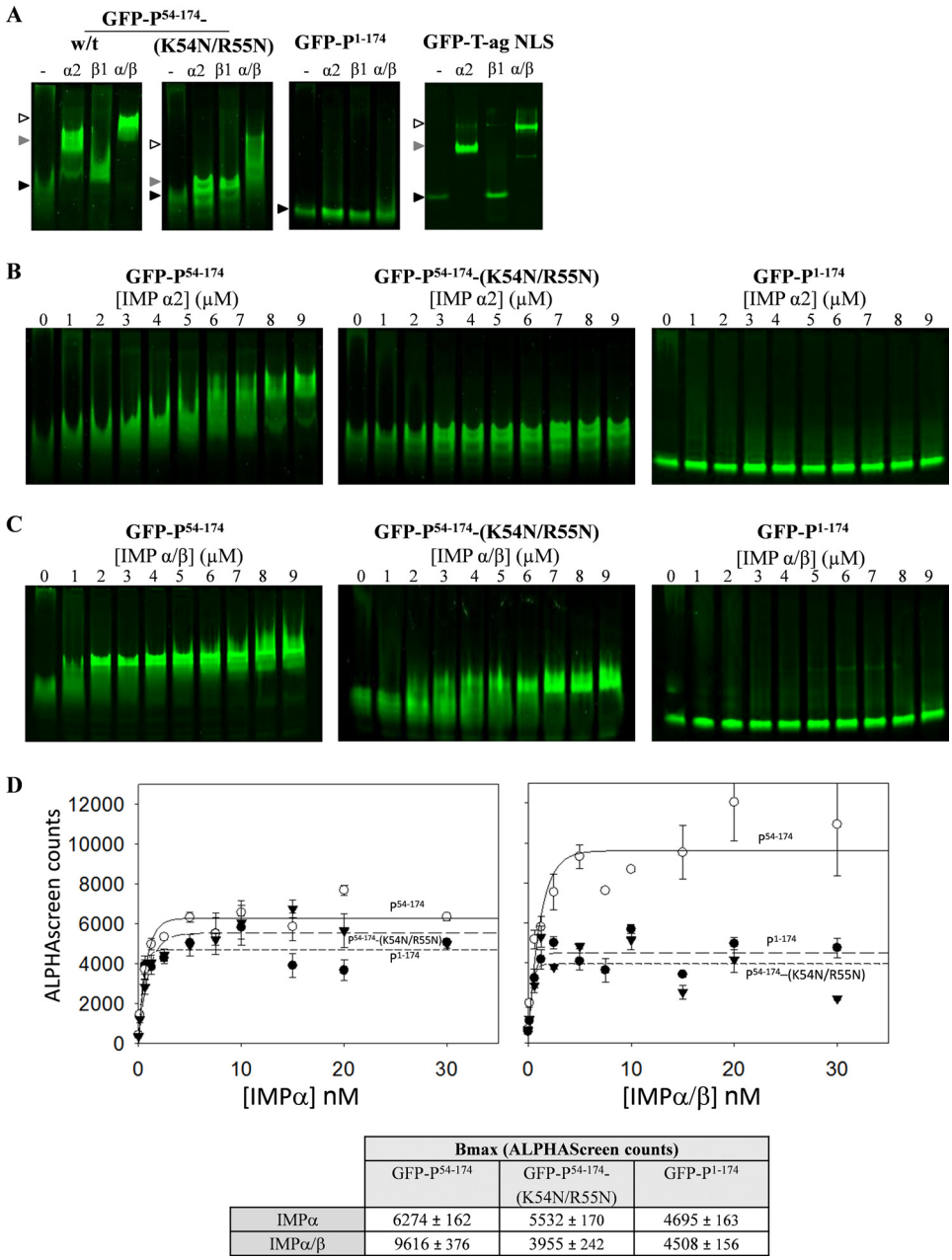

	Bmax (ALPHAScreen counts)		
	GFP-P54-174	GFP-P54-174-(K54N/R55N)	GFP-P1-174
IMPα	6274 ± 162	5532 ± 170	4695 ± 163
IMPα/β	9616 ± 376	3955 ± 242	4508 ± 156

FIGURE 5. **IMPα and α/β binding by P^{54-174} requires residues Lys^{54} and Arg^{55} and is inhibited by residues P^{1-53}.** *A*, the indicated recombinant His_6-tagged GFP-RabV P protein derivatives or GFP-T-ag NLS (2 μM) were incubated without (−) or with 10 μM GST-IMPα2, GST-IMPβ1, or preformed heterodimers of GST-IMPα2/β1 for 15 min, before electrophoresis on a nondenaturing gel, and imaging. Interaction of GFP-RabV P protein derivatives or GFP-T-ag NLS with IMPs is indicated by altered mobility ("shift") of the GFP band compared with the no IMP control (−); *black arrows* indicate non-IMP-associated protein; *gray arrows*, IMPα-associated protein; and *white-filled arrows*, IMPα/β-associated protein. *B* and *C*, GFP-RabV P protein derivatives (2 μM) were incubated with the indicated concentration of GST-IMPα2 (*B*) or GST-IMPα/β heterodimer (*C*) before electrophoresis. *D*, *upper*, the indicated His_6-tagged GFP-P-protein derivatives were incubated with different concentrations of biotinylated IMPα2 or biotinylated IMPα/β heterodimer before conjugation to nickel chelate-coated donor beads and streptavidin-coated acceptor beads for AlphaScreen analysis (51). AlphaScreen assays were performed in triplicate and data (mean AlphaScreen count ± S.E. (*error bars*)) are from a single assay representative of three separate assays. The maximal binding (B_{max}) values (± S.E.) from the curve fits for are shown in the table (*D*, *lower*).

resents a novel and highly efficient strategy to control protein nucleocytoplasmic localization.

Because of the close proximity of P^{1-52} to the critical N-NLS residues Lys^{54} and Arg^{55}, the inhibitory effect of this region is likely to be due to direct molecular masking, whereby P^{1-52} interacts with and/or occludes these key residues from recognition by IMPs, as implied by the direct binding studies where P^{1-174} shows low binding to IMPs in contrast to the clear, high affinity binding by P^{54-174} (Fig. 5*D*), but still enables interaction with CRM1. Alternatively, inhibition of the N-NLS may relate to local structural effects due to the presence or absence of P^{1-52}. Indeed, the region P^{53-88} is predicted to be consistent with the flexible, "intrinsically disordered" regions of protein (58) that are believed to enable the formation of diverse molecular interactions (59–61), such that P^{1-52} could significantly impact on molecular interactions formed by this region.

Importantly, we found that the N-NLS is not a classical short monopartite or bipartite sequence, as P^{53-68} or P^{53-81}, which

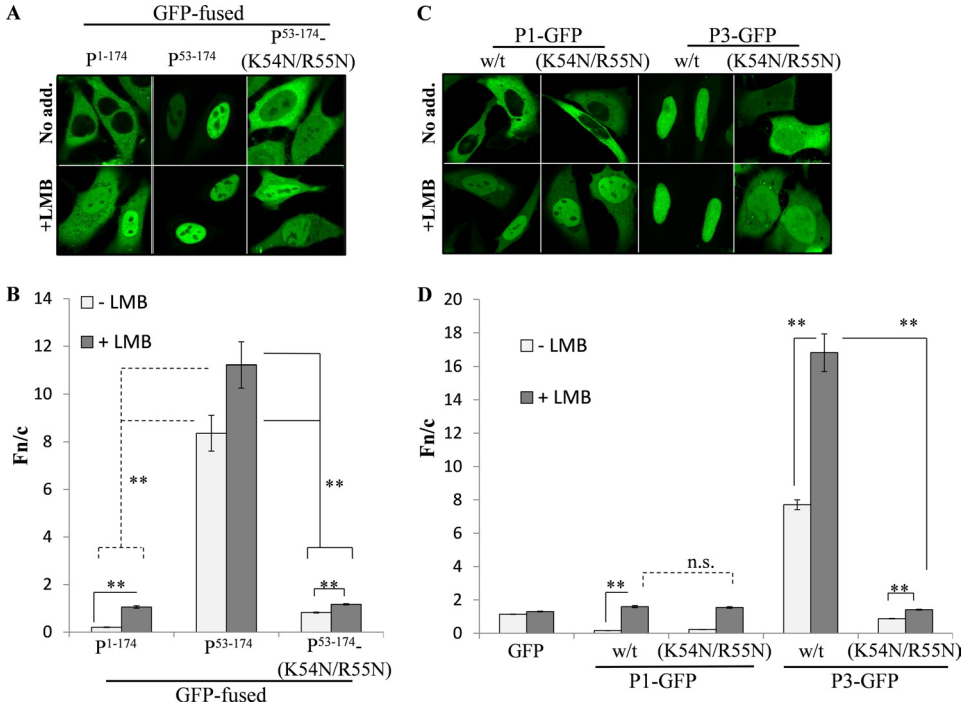

FIGURE 6. **N-NLS activation requires the deletion of P^{1-52}.** *A* and *C*, HeLa cells were transfected to express the indicated proteins and treated with or without LMB. *B* and *D*, analysis of living cells was performed by CLSM to determine the $F_{n/c}$ (mean ± S.E. (*error bars*), $n \geq 73$ from three separate assays) as described in the legend to Fig. 2. Statistical analysis was according to the legend to Fig. 2.

are deleted from P4 and P5 and contain essential N-NLS residues, are not sufficient to recapitulate the nuclear import conferred by P3. In fact, N-NLS activity requires a large region (P^{53-174}) suggestive of an extensive, conformation-dependent signal or a nonclassical bipartite NLS (9, 13) with an unconventionally long spacer region. Several basic residues/motifs in the C-terminal part of P^{53-174} could contribute to such a sequence. Thus, it is possible that regulation of the N-NLS involves broader effects of P^{1-52} on the structure of the P protein. Intriguingly, deletion of P^{1-52} from P3 also appears to be able to activate the microtubule-association sequence (MTAS) within the C-terminal domain (Fig. 1) (43), indicative of such effects on distal regions of P3 and suggesting that the presence or absence of P^{1-52} concomitantly regulates a number of distinct trafficking/regulatory sequences involved in P3-mediated IFN-antagonism (29, 30, 36–38, 42, 43). Importantly, the putative spacer of the N-NLS contains the RabV P dimerization domain (residues 91–131, Fig. 1), structural studies of which indicate the formation of two α-helices that form a hairpin (62) and may thus align distally located residues at the N and C termini of the N-NLS to form a bipartite signal. This is particularly intriguing as the function of the MTAS is dependent on dimerization (43), such that effects on the dimerization domain may contribute to the coordinated effect of the deletion of P^{1-52} on these sequences.

In addition to regulating the activity of the N-NES, N-NLS, and MTAS, residues P^{1-52} also contain sequence critical for binding to the viral polymerase L (P^{1-19}), essential to P1 function as a co-factor in cytoplasmic genome replication/transcription (29). The deletion of this site from isoforms P2–P5 is believed to enable accessory functions, such as antagonism of IFN signaling, which depend on differential subcellular localization (29, 63). Consistent with this hypothesis, recent data indicate that P2, which contains the N-NES and is cytoplasmic, plays a more important role than P1 in inhibiting IFN signaling by arresting STAT1 in the cytoplasm (37, 63, 64). Importantly, our data (this report and see Ref. 43) indicate that the deletion of residues P^{1-52} in P3 does not simply produce a truncated version of P1/P2, but in fact generates a very different protein species, suggesting that this isoform has adopted specific unique properties which enable distinct intranuclear/microtubule-dependent roles in IFN antagonism (29, 35, 37–39, 43). In addition, our finding that nuclear localization of the region P^{53-174} is increased upon treatment with LMB (Fig. 3, *B* and *D*) suggests that this region contains additional NES activity which, together with the DLC-AS (Fig. 4, *C* and *D*), can modulate nuclear localization through the N-NLS. Thus, subcellular trafficking of RabV P isoforms involves complicated and intricate mechanisms, indicating an exquisite requirement for highly regulated nuclear trafficking in RabV infection, presumably to enable efficient shutdown of host immune responses.

In conclusion, we have identified a novel nuclear trafficking module for efficient co-ordinated regulation of the nucleocytoplasmic localization of protein isoforms. Future research will evaluate the role of the N-NLS/N-NES module in the context of infectious virus and pathogenicity *in vivo*, to evaluate its potential as a target for novel antiviral therapeutics/vaccines against RabV, the cause of more than 55,000 human fatalities annually (29, 65). This work should also assist in the delineation of the regulation of trafficking of other cellular and viral protein isoforms to provide important insights into the regulation of proteins involved in diverse cellular pathways and pathological processes.

Acknowledgments—We thank Monash Micro Imaging for providing microscopy instrumentation and technical support and Cassandra David for tissue culture.

REFERENCES

1. Chumakov, S. P., and Prasolov, V. S. (2010) Organization and regulation of nucleocytoplasmic transport. *Mol. Biol.* **44,** 186–201
2. Cook, A., Bono, F., Jinek, M., and Conti, E. (2007) Structural biology of nucleocytoplasmic transport. *Annu. Rev. Biochem.* **76,** 647–671
3. Fulcher, A. J., and Jans, D. A. (2011) Regulation of nucleocytoplasmic trafficking of viral proteins: an integral role in pathogenesis? *Biochim. Biophys. Acta* **1813,** 2176–2190
4. Stewart, M. (2007) Molecular mechanism of the nuclear protein import cycle. *Nat. Rev. Mol. Cell Biol.* **8,** 195–208
5. Poon, I. K., and Jans, D. A. (2005) Regulation of nuclear transport: central role in development and transformation? *Traffic* **6,** 173–186
6. Deonarain, R., Chan, D. C., Platanias, L. C., and Fish, E. N. (2002) Interferon-α/β-receptor interactions: a complex story unfolding. *Curr. Pharm. Des.* **8,** 2131–2137
7. la Cour, T., Kiemer, L., Mølgaard, A., Gupta, R., Skriver, K., and Brunak, S. (2004) Analysis and prediction of leucine-rich nuclear export signals. *Protein Eng. Des. Sel.* **17,** 527–536
8. Ström, A. C., and Weis, K. (2001) Importin-β-like nuclear transport receptors. *Genome Biol.* **2,** REVIEWS3008
9. Lange, A., McLane, L. M., Mills, R. E., Devine, S. E., and Corbett, A. H. (2010) Expanding the definition of the classical bipartite nuclear localization signal. *Traffic* **11,** 311–323
10. Lange, A., Mills, R. E., Lange, C. J., Stewart, M., Devine, S. E., and Corbett, A. H. (2007) Classical nuclear localization signals: definition, function, and interaction with importin α. *J. Biol. Chem.* **282,** 5101–5105
11. Reich, N. C., and Liu, L. (2006) Tracking STAT nuclear traffic. *Nat. Rev. Immunol.* **6,** 602–612
12. Conti, E., Uy, M., Leighton, L., Blobel, G., and Kuriyan, J. (1998) Crystallographic analysis of the recognition of a nuclear localization signal by the nuclear import factor karyopherin? *Cell* **94,** 193–204
13. Giesecke, A., and Stewart, M. (2010) Novel binding of the mitotic regulator TPX2 (target protein for *Xenopus* kinesin-like protein 2) to importin-α. *J. Biol. Chem.* **285,** 17628–17635
14. Hodel, M. R., Corbett, A. H., and Hodel, A. E. (2001) Dissection of a nuclear localization signal. *J. Biol. Chem.* **276,** 1317–1325
15. Kalderon, D., Richardson, W. D., Markham, A. F., and Smith, A. E. (1984) Sequence requirements for nuclear location of simian virus 40 large-T antigen. *Nature* **311,** 33–38
16. Claudiani, P., Riano, E., Errico, A., Andolfi, G., and Rugarli, E. I. (2005) Spastin subcellular localization is regulated through usage of different translation start sites and active export from the nucleus. *Exp. Cell Res.* **309,** 358–369
17. Fagioli, M., Alcalay, M., Pandolfi, P. P., Venturini, L., Mencarelli, A., Simeone, A., Acampora, D., Grignani, F., and Pelicci, P. G. (1992) Alternative splicing of PML transcripts predicts coexpression of several carboxy-terminally different protein isoforms. *Oncogene* **7,** 1083–1091
18. Rodríguez, E., and Martignetti, J. A. (2009) The Krüppel traffic report: cooperative signals direct KLF8 nuclear transport. *Cell Res.* **19,** 1041–1043
19. Chenik, M., Chebli, K., and Blondel, D. (1995) Translation initiation at alternate in-frame AUG codons in the rabies virus phosphoprotein mRNA is mediated by a ribosomal leaky scanning mechanism. *J. Virol.* **69,** 707–712
20. Harcourt, B. H., Tamin, A., Ksiazek, T. G., Rollin, P. E., Anderson, L. J., Bellini, W. J., and Rota, P. A. (2000) Molecular characterization of Nipah virus, a newly emergent paramyxovirus. *Virology* **271,** 334–349
21. Jayakar, H. R., and Whitt, M. A. (2002) Identification of two additional translation products from the matrix (M) gene that contribute to vesicular stomatitis virus cytopathology. *J. Virol.* **76,** 8011–8018
22. Forwood, J. K., Brooks, A., Briggs, L. J., Xiao, C. Y., Jans, D. A., and Vasudevan, S. G. (1999) The 37-amino acid interdomain of Dengue virus NS5 protein contains a functional NLS and inhibitory CK2 Site. *Biochem. Biophys. Res. Commun.* **257,** 731–737
23. Ghildyal, R., Ho, A., Wagstaff, K. M., Dias, M. M., Barton, C. L., Jans, P., Bardin, P., and Jans, D. A. (2005) Nuclear import of the respiratory syncytial virus matrix protein is mediated by importin β1 independent of importin α. *Biochemistry* **44,** 12887–12895
24. Rodriguez, J. J., and Horvath, C. M. (2004) Host evasion by emerging paramyxoviruses: Hendra virus and Nipah virus V proteins inhibit interferon signaling. *Viral Immunol.* **17,** 210–219
25. Rodriguez, J. J., Parisien, J. P., and Horvath, C. M. (2002) Nipah virus V protein evades $\alpha$and γ interferons by preventing STAT1 and STAT2 activation and nuclear accumulation. *J. Virol.* **76,** 11476–11483
26. Rodriguez, J. J., Wang, L. F., and Horvath, C. M. (2003) Hendra virus V protein inhibits interferon signalling by inhibiting STAT-1 and STAT-2 nuclear accumulation. *J. Virol.* **77,** 11842–11845
27. Shaw, M. L., Cardenas, W. B., Zamarin, D., Palese, P., and Basler, C. F. (2005) Nuclear localization of the Nipah virus W protein allows for inhibition of both virus- and Toll-like receptor 3-triggered signaling pathways. *J. Virol.* **79,** 6078–6088
28. Shaw, M. L., García-Sastre, A., Palese, P., and Basler, C. F. (2004) Nipah virus V and W proteins have a common STAT1-binding domain yet inhibit STAT1 activation from the cytoplasmic and nuclear compartments, respectively. *J. Virol.* **78,** 5633–5641
29. Oksayan, S., Ito, N., Moseley, G., and Blondel, D. (2012) Subcellular trafficking in rhabdovirus infection and immune evasion: a Novel target for therapeutics. *Infect. Disord. Drug Targets* **12,** 38–58
30. Pasdeloup, D., Poisson, N., Raux, H., Gaudin, Y., Ruigrok, R. W., and Blondel, D. (2005) Nucleocytoplasmic shuttling of the rabies virus P protein requires a nuclear localization signal and a CRM1-dependent nuclear export signal. *Virology* **334,** 284–293
31. Bouttier, M., Goncalvès, C., Journo, C., Letienne, J., Piña, M., and Vitour, D. (2008) Viruses and interferon: mechanisms of interferon induction and strategies to escape interferon response. *Virologie* **12,** 159–173
32. Davey, N. E., Travé, G., and Gibson, T. J. (2011) How viruses hijack cell regulation. *Trends Biochem. Sci.* **36,** 159–169
33. Gale, M., Jr., and Sen, G. C. (2009) Viral evasion of the interferon system. *J. Interferon Cytokine Res.* **29,** 475–476
34. Ahmed, M., McKenzie, M. O., Puckett, S., Hojnacki, M., Poliquin, L., and Lyles, D. S. (2003) Ability of the matrix protein of vesicular stomatitis virus to suppress β interferon gene expression is genetically correlated with the inhibition of host RNA and protein synthesis. *J. Virol.* **77,** 4646–4657
35. Chelbi-Alix, M. K., Vidy, A., El Bougrini, J., and Blondel, D. (2006) Rabies viral mechanisms to escape the IFN system: the viral protein P interferes with IRF-3, Stat1, and PML nuclear bodies. *J. Interferon Cytokine Res.* **26,** 271–280
36. Ito, N., Moseley, G. W., Blondel, D., Shimizu, K., Rowe, C. L., Ito, Y., Masatani, T., Nakagawa, K., Jans, D. A., and Sugiyama, M. (2010) Role of interferon antagonist activity of rabies virus phosphoprotein in viral pathogenicity. *J. Virol.* **84,** 6699–6710
37. Vidy, A., Chelbi-Alix, M., and Blondel, D. (2005) Rabies virus P protein interacts with STAT1 and inhibits interferon signal transduction pathways. *J. Virol.* **79,** 14411–14420
38. Vidy, A., El Bougrini, J., Chelbi-Alix, M. K., and Blondel, D. (2007) The nucleocytoplasmic rabies virus P protein counteracts interferon signaling by inhibiting both nuclear accumulation and DNA binding of STAT1. *J. Virol.* **81,** 4255–4263
39. Blondel, D., Regad, T., Poisson, N., Pavie, B., Harper, F., Pandolfi, P. P., De Thé, H., and Chelbi-Alix, M. K. (2002) Rabies virus P and small P products interact directly with PML and reorganize PML nuclear bodies. *Oncogene* **21,** 7957–7970
40. Shimizu, K., Ito, N., Mita, T., Yamada, K., Hosokawa-Muto, J., Sugiyama, M., and Minamoto, N. (2007) Involvement of nucleoprotein, phosphoprotein, and matrix protein genes of rabies virus in virulence for adult mice. *Virus Res.* **123,** 154–160
41. Faria, P. A., Chakraborty, P., Levay, A., Barber, G. N., Ezelle, H. J., Enninga, J., Arana, C., van Deursen, J., and Fontoura, B. M. (2005) VSV disrupts the Rae1/mrnp41 mRNA nuclear export pathway. *Mol. Cell* **17,** 93–102
42. Moseley, G. W., Filmer, R. P., DeJesus, M. A., and Jans, D. A. (2007) Nucleocytoplasmic distribution of rabies virus P-protein is regulated by

phosphorylation adjacent to C-terminal nuclear import and export signals. *Biochemistry* **46,** 12053–12061
43. Moseley, G. W., Lahaye, X., Roth, D. M., Oksayan, S., Filmer, R. P., Rowe, C. L., Blondel, D., and Jans, D. A. (2009) Dual modes of rabies P-protein association with microtubules: a novel strategy to suppress the antiviral response. *J. Cell Sci.* **122,** 3652–3662
44. Moseley, G. W., Roth, D. M., DeJesus, M. A., Leyton, D. L., Filmer, R. P., Pouton, C. W., and Jans, D. A. (2007) Dynein light chain association sequences can facilitate nuclear protein import. *Mol. Biol. Cell* **18,** 3204–3213
45. Baliga, B. C., Colussi, P. A., Read, S. H., Dias, M. M., Jans, D. A., and Kumar, S. (2003) Role of prodomain in importin-mediated nuclear localization and activation of caspase-2. *J. Biol. Chem.* **278,** 4899–4905
46. Lahaye, X., Vidy, A., Pomier, C., Obiang, L., Harper, F., Gaudin, Y., and Blondel, D. (2009) Functional characterization of negri bodies (NBs) in rabies virus-infected cells: evidence that NBs are sites of viral transcription and replication. *J. Virol.* **83,** 7948–7958
47. Roth, D. M., Moseley, G. W., Glover, D., Pouton, C. W., and Jans, D. A. (2007) A microtubule-facilitated nuclear import pathway for cancer regulatory proteins. *Traffic* **8,** 673–686
48. Roth, D. M., Moseley, G. W., Pouton, C. W., and Jans, D. A. (2011) Mechanism of microtubule-facilitated "fast track" nuclear import. *J. Biol. Chem.* **286,** 14335–14351
49. Moseley, G. W., Leyton, D. L., Glover, D. J., Filmer, R. P., and Jans, D. A. (2010) Enhancement of protein transduction-mediated nuclear delivery by interaction with dynein/microtubules. *J. Biotechnol.* **145,** 222–225
50. Forwood, J. K., Harley, V., and Jans, D. A. (2001) The C-terminal nuclear localization signal of the sex-determining region Y (SRY) high mobility group domain mediates nuclear import through importin β1. *J. Biol. Chem.* **276,** 46575–46582
51. Wagstaff, K. M., and Jans, D. A. (2006) Intramolecular masking of nuclear localization signals: analysis of importin binding using a novel AlphaScreen-based method. *Anal. Biochem.* **348,** 49–56
52. Wagstaff, K. M., Dias, M. M., Alvisi, G., and Jans, D. A. (2005) Quantitative analysis of protein-protein interactions by native PAGE/fluorimaging. *J. Fluoresc.* **15,** 469–473
53. Kosugi, S., Hasebe, M., Tomita, M., and Yanagawa, H. (2009) Systematic identification of cell cycle-dependent yeast nucleocytoplasmic shuttling proteins by prediction of composite motifs. *Proc. Natl. Acad. Sci. U.S.A.* **106,** 10171–10176
54. Poisson, N., Real, E., Gaudin, Y., Vaney, M. C., King, S., Jacob, Y., Tordo, N., and Blondel, D. (2001) Molecular basis for the interaction between rabies virus phosphoprotein P and the dynein light chain LC8: dissociation of dynein-binding properties and transcriptional functionality of P. *J. Gen. Virol.* **82,** 2691–2696
55. Fulcher, A. J., Dias, M. M., and Jans, D. A. (2010) Binding of p110 retinoblastoma protein inhibits nuclear import of simian virus SV40 large tumor antigen. *J. Biol. Chem.* **285,** 17744–17753
56. Kaur, G., Delluc-Clavieres, A., Poon, I. K., Forwood, J. K., Glover, D. J., and Jans, D. A. (2010) Calmodulin-dependent nuclear import of HMG-box family nuclear factors: importance of the role of SRY in sex reversal. *Biochem. J.* **430,** 39–48
57. Kaur, G., and Jans, D. A. (2011) Dual nuclear import mechanisms of sex determining factor SRY: intracellular Ca^{2+} as a switch. *FASEB J.* **25,** 665–675
58. Gerard, F. C., Ribeiro Ede, A., Jr., Leyrat, C., Ivanov, I., Blondel, D., Longhi, S., Ruigrok, R. W., and Jamin, M. (2009) Modular organization of rabies virus phosphoprotein. *J. Mol. Biol.* **388,** 978–996
59. Uversky, V. N. (2011) Intrinsically disordered proteins from A to Z. *Int. J. Biochem. Cell Biol.* **43,** 1090–1103
60. Uversky, V. N., Shah, S. P., Gritsyna, Y., Hitchcock-DeGregori, S. E., and Kostyukova, A. S. (2011) Systematic analysis of tropomodulin/tropomyosin interactions uncovers fine-tuned binding specificity of intrinsically disordered proteins. *J. Mol. Recognit.* **24,** 647–655
61. Xue, B., Williams, R. W., Oldfield, C. J., Goh, G. K., Dunker, A. K., and Uversky, V. N. (2010) Viral disorder or disordered viruses: do viral proteins possess unique features? *Protein Pept. Lett.* **17,** 932–951
62. Ivanov, I., Crépin, T., Jamin, M., and Ruigrok, R. W. (2010) Structure of the dimerization domain of the rabies virus phosphoprotein. *J. Virol.* **84,** 3707–3710
63. Marschalek, A., Drechsel, L., and Conzelmann, K. K. (2012) The importance of being short: the role of rabies virus phosphoprotein isoforms assessed by differential IRES translation initiation. *Eur. J. Cell Biol.* **91,** 17–23
64. Brzózka, K., Finke, S., and Conzelmann, K. K. (2006) Inhibition of interferon signaling by rabies virus phosphoprotein P: activation-dependent binding of STAT1 and STAT2. *J. Virol.* **80,** 2675–2683
65. Schnell, M. J., McGettigan, J. P., Wirblich, C., and Papaneri, A. (2010) The cell biology of rabies virus: using stealth to reach the brain. *Nat. Rev. Microbiol.* **8,** 51–61
66. Raux, H., Flamand, A., and Blondel, D. (2000) Interaction of the rabies virus P protein with the LC8 dynein light chain. *J. Virol.* **74,** 10212–10216
67. Chenik, M., Chebli, K., Gaudin, Y., and Blondel, D. (1994) *In vivo* interaction of rabies virus phosphoprotein (P) and nucleoprotein (N): existence of two N-binding sites on P protein. *J. Gen. Virol.* **75,** 2889–2896
68. Chenik, M., Schnell, M., Conzelmann, K. K., and Blondel, D. (1998) Mapping the interacting domains between the rabies virus polymerase and phosphoprotein. *J. Virol.* **72,** 1925–1930